MAPPING SNOW ALGAE CONCENTRATION IN THE SIERRA NEVADA WITH IMAGING SPECTROSCOPY

Thomas H. Painter[1], Brian Duval[2], William H. Thomas[3], Maria Mendez[3], Sarah Heintzelman[3], and Jeff Dozier[4]

ABSTRACT

We present spectral reflectance measurements of algal snow and a model to retrieve snow algal concentration from imaging spectrometer data collected in the Tioga Pass region of the Sierra Nevada, California. Spectral reflectance measurements of snow containing the algae *Chlamydomonas Nivalas* exhibit carotenoid absorption in the wavelength range 0.4 – 0.58 μm and chlorophyll-*a,-b* absorption in the wavelength range 0.6 – 0.7 μm. The integral of the scaled chlorophyll-*a,-b* absorption feature , I_{680}, varies with algal concentration, C_a. The relationship appears to be exponential but this model is not yet statistically significant due to limited data at high concentrations. Using the relationship, $C_a = 922.61\ exp(13.56\ I_{680})$, we inverted Airborne Visible Imaging Spectrometer (AVIRIS) data for algae concentration. In the 5.5 km^2, imaged region, the mean algal concentration was 880 cells/mL with a standard deviation of 1445 cells/mL. We calculated the total imaged algal biomass, B_a = 11.1 kg. From the field spectral measurements, we fit a model relating snow albedo, A_s, to C_a. We inverted algae concentration images for albedo using this model. Mean retrieved albedo was 0.595 with a standard deviation of 0.009, a minimum of 0.43, and a maximum of 0.62.

INTRODUCTION

The biological, physical, and optical properties of snow algae have been studied at the plot scale by many authors (Thomas 1972; Thomas and Duval 1995; Hoham 1998). Thomas (1972) studied the spatial and stratigraphic distribution of snow algae at the scale of the Sierra Nevada, California. To date, the spatial distribution of snow algae at the basin scale remains unexplored. Remote sensing, and in particular imaging spectroscopy, offers the capacity to analyze spectral reflectance features that are related to snow algae concentration.

Chlamydomonas nivalis represents the most prevalent alga found in snowpacks in the Sierra Nevada of California. The generally accepted life cycle model for red snow alga has that in the fall, alga spores lie dormant on the surface after complete snow ablation. In winter, spores still lie dormant under a deepening snowpack. In late spring, snowmelt fills a sufficient fraction of the pore space to allow a continuous path of liquid water from the substrate to the snow-air interface. Algae release green flagellated stages that swim up through this liquid water path to or near the surface. In response to increasing UV and/or visible radiation, red spores are formed that concentrate in a red bloom at the surface.

Thomas (1972) described reports of red snow in California from as early as 1871. The first report of red snow at Tioga Pass came from Sharsmith (1935). Algae exist in snowfields on all continents with the first observation in Africa coming in 1998 in the Atlas Mountains (Kol 1968; Duval et al. 1999). In the Sierra Nevada, California, snow algae are found in old, wet snowfields at elevations > 3000 m. During bloom, most cells lie near the snow-air interface but can be found down to depths of 10 cm (Thomas 1972). Thomas and Duval (1995) demonstrated significant negative correlation between snow albedo and algal cell concentration but also found that decreases in albedo by algal snow did not contribute to a significant decrease in the mean albedo of snowfields. Yoshimura et al. (2000) demonstrated the use of algal layers for dating ice cores in Himalayan glaciers.

This work attempts to address multiple unexplored problems. The first is document and analyze the reflectance spectrum of algal snow and its relation to algal concentration. The second goal is to develop a model that relates algal concentration to the reflectance spectrum of algal snow. The third goal was to assess the ability of remote sensing with an imaging spectrometer to detect and quantify the spatial distribution of algal concentration in alpine snow. The final goal is to analyze the spatial distribution of snow albedo and its relationship with algal concentration.

Paper presented at the 69th Annual Meeting of the Western Snow Conference, 2001.

[1]Institute for Computational Earth System Science, University of California, Santa Barbara, California

[2]Massachusetts Dept. of Environmental Protection, Worcester, Massachusetts

[3]Scripps Institute of Oceanography, La Jolla, California

[4]Donald Bren School of Environ. Sci. and Management, University of California, Santa Barbara, California

METHODS

Site

Our field site lies just outside the eastern boundary of Yosemite National Park, California near Tioga Pass (37°55'N, 119°16'W). Snowfields near Saddlebag Lake exhibit an annual algal bloom that some of the authors have studied for many years. Elevation in the Mt. Conness basin ranges from 3050 to 3800 m.

The site lies entirely above timberline and surface cover consists of granite slabs, tundra-covered soils, and willows. The mean accumulation on April 1 in snow water equivalent at the California Cooperative Snow Survey Saddlebag Lake site is 31.2". While the Sierra Nevada is considered to have a predominantly maritime snow regime, some regions on the eastern Sierra exhibit intermountain characteristics. Snow algae in this region usually commence their red bloom in late-May to early-June (Thomas 1972; Thomas and Duval 1995). In the summer of 2000, when the data presented here were collected, the algal bloom had commenced before June 20.

Snow Spectral Reflectance

We measured the spectral reflectance of snow in the field with an Analytical Spectral Devices (Boulder, CO) FR field spectroradiometer. The FR records digital numbers at 2151 spectral bands across the wavelength range 0.35 – 2.5 μm in a dynamic range that is automatically optimized for current light conditions. We collect spectra of a near-100% reflectance Spectralon white panel (*Labsphere*, New Sutton, NH) laid parallel to the surface and immediately after, collect spectra of the snow target. Both sets of measurements are made with a view angle that is normal to the surface in order to maintain consistency in bi-directional reflectance across all samples. Spectral reflectance, R_λ, is calculated as:

$$(1)\quad R_\lambda = WRC_\lambda \frac{DN_{snow,\lambda}}{DN_{white,\lambda}}$$

where $DN_{snow,\lambda}$ is the digital number measured from the snow target at wavelength λ, $DN_{white,\lambda}$ is the spectral digital number of the white reflectance standard, and WRC_λ is the calibration coefficient for the white reflectance standard. Measured as such and assuming that the white reflectance standard is a Lambertian target, R_λ is the equivalent of the nadir bi-directional reflectance factor for the given solar geometry (Schott 1998).

Algal Concentration

We determine algal concentration, C_a, by collecting snow samples in the field and processing in the laboratory. Snow samples were collected in Whirl-Pak™ bags with 100 mL capacity. We returned melted samples at day's end to the Sierra Nevada Aquatic Research Laboratory (SNARL) at Mammoth Lakes, CA. Under the microscope, we count the number of algal cells per fixed volume. We collected 26 snow samples from which we measured spectral reflectance, 13 of which were for algal snow (observed to be reddish) and 13 of which were for algal-free snow (observed to be void of red).

Imaging Spectrometer Data

We used data from the NASA/JPL Airborne Visible Infrared Imaging Spectrometer (AVIRIS). AVIRIS measures reflected radiance in 224 bands across the wavelength range 0.4 – 2.5 μm at 0.01 μm spectral resolution and a 1 mrad field-of-view. The usual platform for AVIRIS is the NASA ER-2 that flies at 20 km producing a nominal spatial resolution of 20 m. For our acquisition, AVIRIS was mounted on a Twin Otter flying at 4.4 km giving a spatial resolution of 1.2 m given a mean surface elevation of 3.2 km.

AVIRIS data are delivered as calibrated radiance with units of μW/cm^2/nm/sr. We convert calibrated radiance to apparent surface reflectance using a non-linear least squares model that fits water vapor absorption in the AVIRIS data (Green et al. 1993). Apparent surface reflectance, ASR_λ, is defined as

$$(2)\quad ASR_\lambda = \frac{L_{AVI,\lambda}}{(E_\lambda / \pi)} = \frac{\pi L_{AVI,\lambda}}{E_\lambda}$$

where $L_{AVI,\lambda}$ is the AVIRIS measured radiance at wavelength λ and E_λ is the irradiance on a level surface at the mean surface elevation as modeled with the MODTRAN3.5 atmospheric transmission model (Berk et al. 1989).

RESULTS

Snow Spectral Reflectance

Figure 1 shows the spectral reflectance for algal-free and algal snow. The algal-free reflectance spectrum is characterized by high reflectance in the visible wavelengths, moderate reflectance in the wavelength range $0.7 \leq \lambda \leq 1.4$ μm, and very low reflectance in the wavelength range $1.4 \leq \lambda \leq 2.5$ μm (Warren 1982). The algal snow reflectance spectrum has moderate, concave reflectance in the visible wavelengths due to absorption by carotenoids

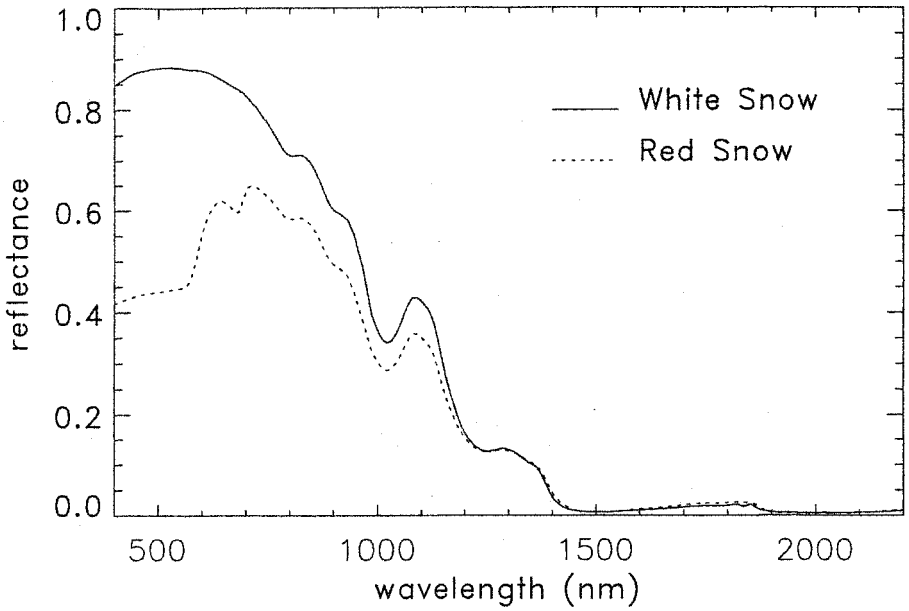

Figure 1 Spectral reflectance measurements for algae-free snow (white) and algal snow (red), measured near Saddlebag Lake, CA with ASD-FR field spectroradiometer.

($0.4 \leq \lambda \leq 0.64$ μm) and a local reflectance minimum at 0.68 μm due to chlorophyll-*a,-b* absorption. Both reflectance spectra exhibit local reflectance minima that correspond to ice absorption features. The carotenoid and chlorophyll absorption features offer leverage to detect algal snow. However, at lower algal concentrations (< ~5000 cells/mL) the carotenoid feature can resemble the effects of dirt on the reflectance spectrum of snow and thus confound a model for detecting algal snow. However, the chlorophyll absorption feature at $\lambda \cong 0.68$ μm is uniquely biological. Therefore, we focused our efforts on this feature.

In Figure 2, we show the normalized reflectance spectra of snow with varying algal concentration. The 0.68 μm absorption feature properly consists of chlorophyll-*a* absorption centered at 0.68 μm and chlorophyll-*b* absorption centered at 0.65 μm, dominated by the former. The depth and breadth of the 0.68 μm absorption feature increase with increasing algal concentration. We used a technique for analysis of absorption features introduced by Clark and Roush (1984) for mineral applications and used by Nolin and Dozier (2000) to retrieve snow grain size. The method relates the integral of the absorption feature, scaled by its continuum, to the physical parameter, in this case the algal concentration. The scaled integral is given by

$$(3)\quad I_{0.68} = \int_{0.63\mu m}^{0.70\mu m} \frac{R_{cont,\lambda} - R_{snow,\lambda}}{R_{cont,\lambda}} d\lambda$$

where $R_{cont,\lambda}$ is the reflectance of the continuum spectrum at wavelength λ and $R_{snow,\lambda}$ is the reflectance of the snow spectrum at wavelength λ. Scaling by the inverse of the continuum reflectance accounts for changes in irradiance and thereby gives an accurate measure of the relative absorption.

Plotting C_a versus $I_{0.68}$ shows an exponential relationship (Figure 3). However, if the highest concentration is removed from the plot, the relationship appears linear. The optical physics of scattering and absorption by impurities in snow would suggest that an exponential relationship is appropriate. However, with only one sample at very high concentrations, we cannot resolve this relationship with statistical significance. For this work, we

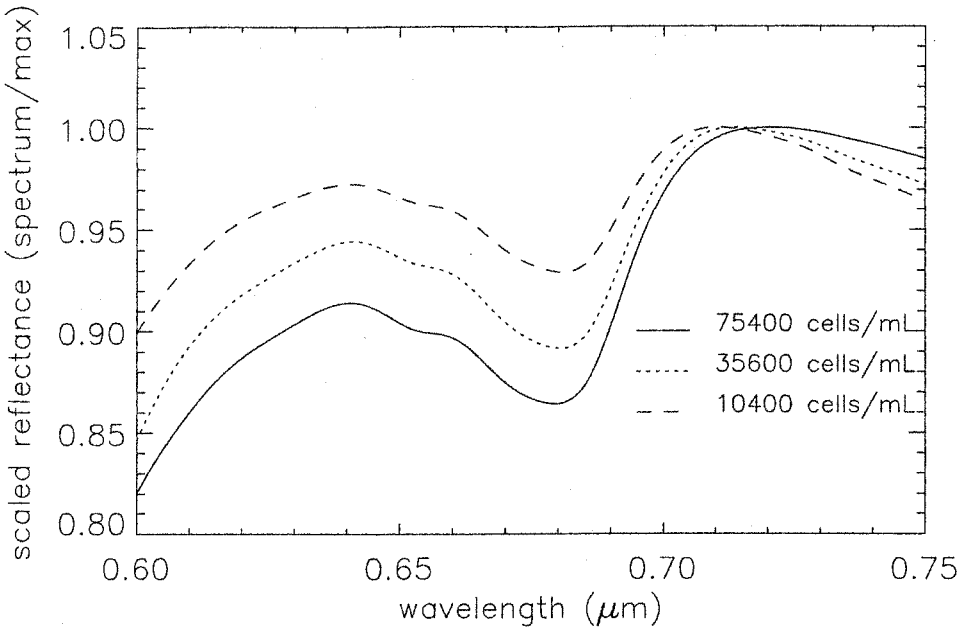

Figure 2 Normalized spectral reflectance of algal snow for varying algal concentration. The depth and breadth of the absorption feature at 0.68 μm increase as C_a increase.

assumed the exponential relationship with the explicit understanding that estimates of C_a may be overestimated at higher concentrations. This relationship is given by

(4) $C_a = 922.61\, e^{13.56 I_{0.68}}$

Ultimately, either assumption produces approximately the same results because for these AVIRIS data $0 \leq I_{0.68} \leq 0.25$ which lie in the relatively linear portion of the plot.

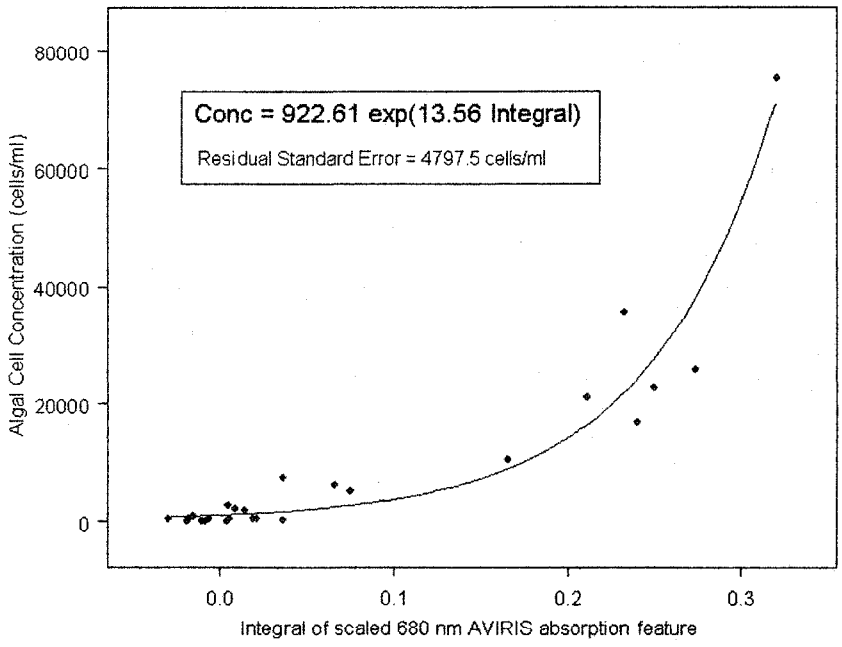

Figure 3 Lab-sampled algal cell concentration (cells/mL) plotted against the integral of the continuum-scaled 0.68 mm chlorophyll absorption feature. The data suggest an exponential relationship but would suggest a strong linear relationship if we remove the sample with the highest algal cell concentration. An exponential relationship is consistent with the physics describing a moderately absorbing medium lying in a multiple-scattering, weekly-absorbing medium such as snow.

Figure 4 AVIRIS radiance image with band center wavelength of $\lambda = 0.635$ μm near Saddlebag Lake, CA. The image was acquired on July 19, 2000. The AVIRIS pixel size is 1.2 m. North is at the top of the image. The masked areas along the left and right edges accommodate the spatial span of the data necessary for georectification. Georectification was performed to correct for changes in the plane attitude. Snowfields are apparent as white patches, spectrally distinct from the other surface cover which is predominantly exposed granite slab.

Algal Concentration and Biomass

Figure 4 shows a single band radiance AVIRIS image from the Saddlebag Lake flightline. The results of applying equation (4) to the AVIRIS apparent surface reflectance data are shown in Figure 5. This image is a 1/9th subset of the total flight line. The vast majority of snowfields in this image lie on north facing slopes. These data show contiguous patches of algal snow, highest concentrations lying near the feet of snowfields. This is consistent with observations made in the field in summer, 2000 and earlier observations (Thomas 1972; Thomas and Duval 1995). The mean C_a for the imaged region was 880 cells/mL with a standard deviation of 1179 cells/mL, and a range of 0 to 123,000 cells/mL. The maximum value retrieved is well beyond the range of apparent validity of equation (4). The total snow-covered area in the image is 0.495 km^2, ~9% of the total 5.5 km^2 imaged area.

Under the assumption that all of the algal biomass lies in the top 10 cm of snow and that our estimates of algal concentration represent the mean of the top 10 cm (Thomas 1972), we can estimate the total imaged biomass, B_a. The general calculation is given by

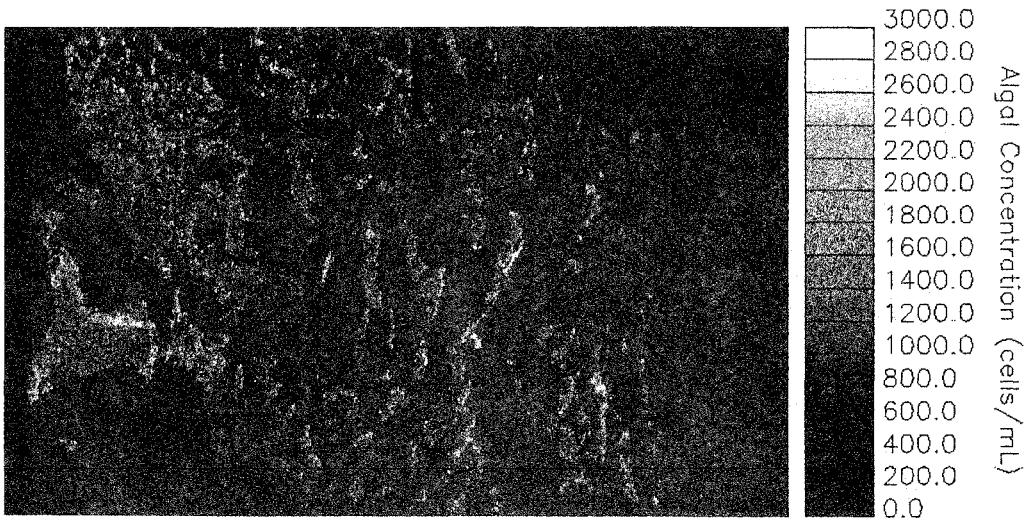

Figure 5 Snow algal concentration (cells/mL) retrieved from AVIRIS apparent surface reflectance data with the model described with equation (4). Snow-free areas have been masked from analysis.

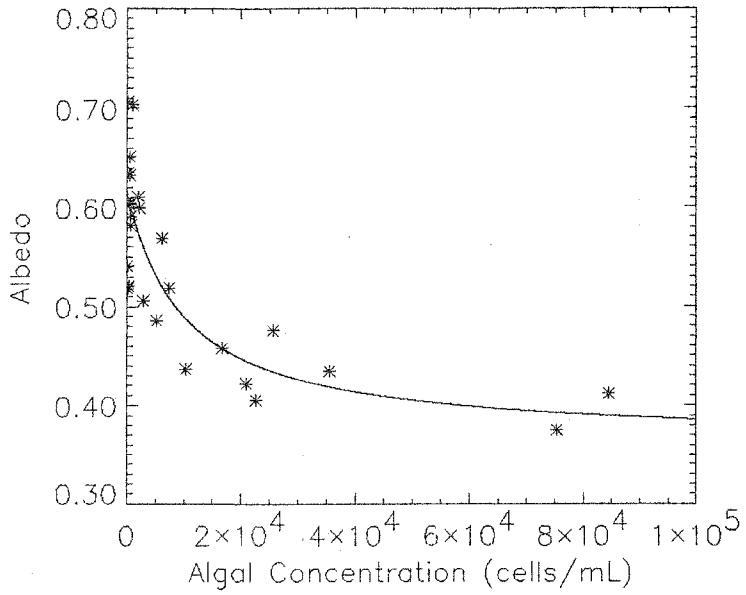

Figure 6 Snow albedo plotted against snow algal concentration for the 26 snow samples collected near Saddlebag Lake. The scatter is fit with inverse relation given in equation (7).

$$(5)\quad B_a = \frac{C_a A d \rho_s N_s m_a}{\rho_w}$$

where A is the mean AVIRIS pixel area, d is the snow depth in which the algae lie, ρ_s is the snow density (kg/m^3), N_s is the number of snow covered pixels in the AVIRIS image, m_a is the mass of an algal cell (kg), and ρ_w is the density of liquid water.

For this AVIRIS flight line, C_a = 880 cells/mL, A = (1.2)^2 m^2, d = 0.1 m, ρ_s = 456 kg/m^3 (measured in the field), N_s = 343,554 pixels, m_a = 0.00056 µg/cell (Thomas 1972), and ρ_w = 1000 kg/m^3, resulting in B_a = 11.1 kg. Given a snow-covered area in the image of 0.495 km^2, the spatial concentration is 0.022 g/m^2.

Snow Albedo

To estimate snow albedo, we first used the atmospheric transmission model SBDART (Ricchiazzi et al. 1998) to determine the spectral irradiance at the surface in this region at the time of acquisition for our samples. We then convolved spectral irradiance with the measurements of spectral reflectance as follows to give albedo:

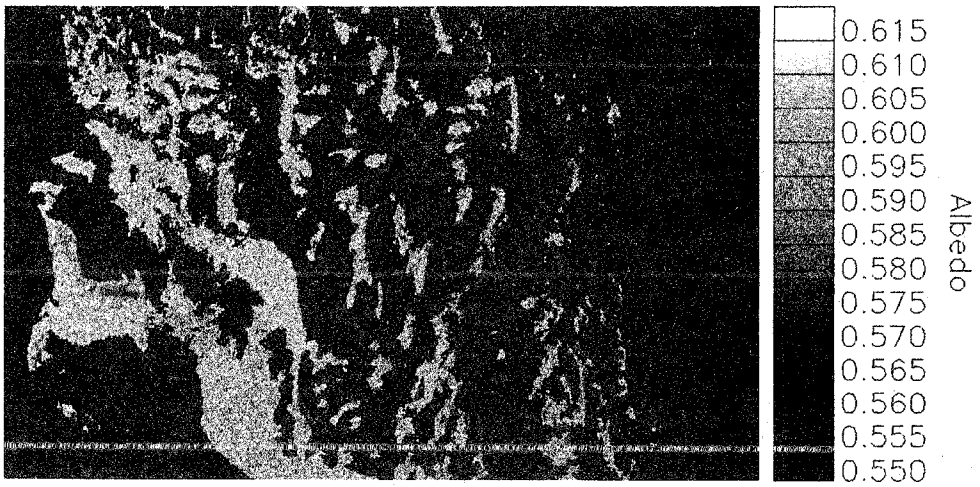

Figure 7 Snow albedo retrieved from algal concentration (Figure 5) using the model represented by equation (7). Snow-free areas have been masked from analysis.

$$(6)\quad A_s = \frac{\int_{\lambda} E_\lambda R_\lambda}{\int_{\lambda} E_\lambda}$$

where E_λ is the spectral irradiance and R_λ is spectral reflectance as discussed above.

Figure 6 shows the albedo estimates using equation (6) for our 26 field samples plotted against the respective measured algal concentration. The plot exhibits an inverse relationship that we fit with the following equation

$$(7)\quad A_s = \frac{2515.13}{(C_a + 9967.12)} + 0.363.$$

Applying equation (7) to the image of algal concentration shown in Figure 5 gives the spatial distribution of snow albedo as shown in Figure 7.

The mean retrieved albedo was 0.595 with a standard deviation of 0.009, a maximum of 0.62, and a minimum of 0.43. If we remove the pixels for which A < 0.58, the mean retrieved albedo is still 0.596 with a standard deviation of 0.006. Hence, while snow algae reduce the plot scale albedo, the basin scale albedo is unaffected for the given spatial distribution of snow algae concentration. This result is consistent with the conclusions by Thomas and Duval (1995) that snow algae does not affect the basin-scale albedo of snowfields.

CONCLUSIONS

We have demonstrated the capacity of imaging spectroscopy to map the spatial distribution of snow algal concentration. The spectral reflectance signature of algal snow exhibits absorption by carotenoids for wavelengths $\lambda \leq 0.6$ μm and chlorophyll-*a* and chlorophyll-*b* absorption in the wavelength range $0.63 \leq \lambda \leq 0.70$ μm. From field spectral reflectance measurements, we developed a model relating algal concentration to the scaled integral of the chlorophyll absorption feature. Applying this model to reflectance data acquired over the east drainages of Mt. Conness near Tioga Pass, California, with the Airborne Visible Infrared Imaging Spectrometer (AVIRIS), we mapped the spatial distribution of snow algal concentration.

The mean inferred algal concentration was 880 cells/mL with a standard deviation of 1179 cells/mL, a minimum of 0 cells/mL, and a maximum of 123,000 cells/mL. Assuming the algal biomass lies in the top 10 cm of the snowpack, we estimated a total imaged algal biomass of 11.1 kg. The total snow-covered area was 0.495 km^2, so the areal biomass concentration was 0.02 g/m^2.

We calculated snow albedo for our field samples with the spectral reflectance measurements and the solar spectral irradiance at the surface as modeled with the atmospheric transmission model SBDART. Albedo is inversely related to algal concentration as would be expected from the relationship between algal concentration and chlorophyll absorption. Applying a model relating albedo to algal concentration to the image of algal concentration, we mapped the spatial distribution of snow albedo. The mean retrieved albedo was 0.595 with a standard deviation of 0.009. While snow algae reduce the albedo at the scale of a few pixels, the basin scale albedo is relatively unaffected for this spatial distribution of snow algae concentration.

The relationship between algal concentration and the scaled integral of the 0.68 μm absorption feature appears to be exponential but would be linear if the point with the highest concentration is removed. Therefore, further measurements of spectral reflectance for high algal concentrations are needed to resolve this relationship. Measurements of the spatial variability of algal concentration at the sub-pixel scale will be made to understand the scales of spatial variability. We are scheduled to acquire more AVIRIS data over the same sites in summer, 2001. From these data, we may begin to address the inter-annual variability of the spatial distribution of snow algae.

ACKNOWLEDGMENTS

Funding for this research came from NASA Grant NAG5-4814 (EOS IDS "Hydrology, Hydrochemistry, and Remote Sensing in Seasonally Snow Covered Alpine Drainage Basins") and the Scripps Vetlesen Grant "Variations in Sierra Nevada Snow Algae Abundances and Nutrient Chemistry in Relation to Global Change". We thank Dan Dawson of the Sierra Nevada Aquatic Research Laboratory (SNARL) in Mammoth Lakes, CA for assistance. We thank Maura Longden, District Ranger for Tuolumne Meadows in Yosemite National Park, CA for being a generous hostess.

REFERENCES

Berk, A., L.S. Bernstein, and D.C. Robertson. 1989. MODTRAN: A Moderate Resolution Model for LOWTRAN 7. *Air Force Geophysics Laboratory Technical Report GL-TR-89-0122*. Hanscom AFB, MA.

Clark, R.N., and T. L. Roush. 1984. Reflectance spectroscopy: quantitative analysis techniques for remote sensing applications. *Journal of Geophysical Research* 89(B7):6329-40.

Duval, B., E. Duval, and R. W. Hoham. 1999. Snow algae of the Sierra Nevada, Spain, and High Atlas mountains of Morocco. *International Microbiology* 2:39-42.

R. O. Green, J. E. Conel, and D. A. Roberts. 1993. Estimation of aerosol optical depth and calculation of apparent surface reflectance from radiance measured by the Airborne Visible Infrared Imaging Spectrometer (AVIRIS) using MODTRAN2. SPIE Conf. No. 1937. *Imaging spectrometry of the terrestrial environment.* p.12.

Hoham, R. W., E. M. Schlag, J. Y. Kang, A. J. Hasselwander, A. F. Behrstock, I. R. Blackburn, R. C. Johnson, and S. C. Roemer. 1998. The effects of irradiance levels and spectral composition on mating strategies in the snow alga, *Chloromonas* sp.-D, from the Tughill Plateau, New York State. *Hydrological Processes* 12:1627-1639.

Kol, E.. 1968. Kryobiologie. Biologie und limnologie des Schnees und Eises. I. Kryovegetation. In: Elster H.j., Ohle, W., eds.. Die Binnengewasser. Stuttgart: E. Schweizerbart'sche Verlagbuchhandlung. 216pp.

Nolin, A. W., and J. Dozier. 2000. A hyperspectral method for remotely sensing the grain size of snow. *Remote Sensing of Environment* 74(N2):207-216.

Ricchiazzi, P., S.R. Yang, C. Gautier, and D. Sowle. 1998. SBDART: A research and teaching software tool for plane-parallel radiative transfer in the Earth's atmosphere. *Bulletin Of The American Meteorological Society* 79(10):2101-2114.

Schott, J. R.. 1997. Remote Sensing: The Image Chain Approach. Oxford University Press. Oxford, U.K.

Sharsmith. 1935. Red snow at Tioga Pass. *Yosemite Nature Notes* 14:63.

Thomas, W. H. 1972. Observations on snow algae in California. *Journal of Phycology* 19:200-204.

Thomas, W. H., and B. Duval. 1995. Sierra Nevada, California, USA, Snow algae – snow albedo changes, algal bacterial interrelationships, and ultraviolet radiation effects. *Arctic and Alpine Research* 27(N4):389-399.

Warren, S. G. 1982. Optical Properties of Snow. *Reviews of Geophysics and Space Physics* 20(1):67-89.

Yoshimura, Y.; S. Kohshima; N. Takeuchi; K. Seko; and K. Fujita. 2000. Himalayan ice-core dating with snow algae. *Journal of Glaciology* 46(N153):335-340.